

Growth of high-crystallinity uniform GaAs nanowire arrays by molecular beam epitaxy

Yu-Bin Kang(亢玉彬), Feng-Yuan Lin(林逢源), Ke-Xue Li(李科学), Ji-Long Tang(唐吉龙),Xiao-Bing Hou(侯效兵), Deng-Kui Wang(王登魁), Xuan Fang(方铉), Dan Fang(房丹),Xin-Wei Wang(王新伟), and Zhi-Peng Wei(魏志鹏)
Citation: Chin. Phys. B, 2021, 30 (**7**): 078102. DOI: 10.1088/1674-1056/abf920
Journal homepage: http://cpb.iphy.ac.cn; http://iopscience.iop.org/cpb

What follows is a list of articles you may be interested in

Effect of growth temperature of $GaAs_xSb_{1-x}$ metamorphic buffer layer on electron mobility of InAs/AlSb heterostructures grown on Si substrate

Jing Zhang(张静), Hong-Liang Lv(吕红亮), Hai-Qiao Ni(倪海桥), Shi-Zheng Yang(杨施政), Xiao-Ran Cui(崔晓然), Zhi-Chuan Niu(牛智川), Yi-Men Zhang(张义门), Yu-Ming Zhang(张玉明)
Chin. Phys. B, 2019, 28 (**11**): 118102. DOI: 10.1088/1674-1056/ab4d49

Molecular beam epitaxial growth of high quality InAs/GaAs quantum dots for 1.3-μ quantum dot lasers

Hui-Ming Hao(郝慧明), Xiang-Bin Su(苏向斌), Jing Zhang(张静), Hai-Qiao Ni(倪海桥), Zhi-Chuan Niu(牛智川)
Chin. Phys. B, 2019, 28 (**7**): 078104. DOI: 10.1088/1674-1056/28/7/078104

1.3-μm InAs/GaAs quantum dots grown on Si substrates

Fu-Hui Shao(邵福会), Yi Zhang(张一), Xiang-Bin Su(苏向斌), Sheng-Wen Xie(谢圣文), Jin-Ming Shang(尚金铭), Yun-Hao Zhao(赵云昊), Chen-Yuan Cai(蔡晨元), Ren-Chao Che(车仁超), Ying-Qiang Xu(徐应强), Hai-Qiao Ni(倪海桥), Zhi-Chuan Niu(牛智川)
Chin. Phys. B, 2018, 27 (**12**): 128105. DOI: 10.1088/1674-1056/27/12/128105

Short-wave infrared InGaAs photodetectors and focal plane arrays

Yong-Gang Zhang(张永刚), Yi Gu(顾溢), Xiu-Mei Shao(邵秀梅), Xue Li(李雪), Hai-Mei Gong(龚海梅), Jia-Xiong Fang(方家熊)
Chin. Phys. B, 2018, 27 (**12**): 128102. DOI: 10.1088/1674-1056/27/12/128102

Novel graphene enhancement nanolaser based on hybrid plasmonic waveguides at optical communication wavelength

Zhengjie Xu(徐政杰), Jun Zhu(朱君), Wenju Xu(徐汶菊), Deli Fu(傅得立), Cong Hu(胡聪), Frank Jiang
Chin. Phys. B, 2018, 27 (**8**): 088104. DOI: 10.1088/1674-1056/27/8/088104

Growth of high-crystallinity uniform GaAs nanowire arrays by molecular beam epitaxy*

Yu-Bin Kang(亢玉彬)[1], Feng-Yuan Lin(林逢源)[1,†], Ke-Xue Li(李科学)[1], Ji-Long Tang(唐吉龙)[1,‡], Xiao-Bing Hou(侯效兵)[1], Deng-Kui Wang(王登魁)[1], Xuan Fang(方铉)[1], Dan Fang(房丹)[1], Xin-Wei Wang(王新伟)[2], and Zhi-Peng Wei(魏志鹏)[1]

[1] *State Key Laboratory of High Power Semiconductor Lasers, Changchun University of Science and Technology, Changchun* 130022, *China*
[2] *School of Materials Science and Engineering, Changchun University of Science and Technology, Changchun* 130022, *China*

(Received 3 March 2021; revised manuscript received 30 March 2021; accepted manuscript online 19 April 2021)

The self-catalyzed growth of GaAs nanowires (NWs) on silicon (Si) is an effective way to achieve integration between group III–V elements and Si. High-crystallinity uniform GaAs NW arrays were grown by solid-source molecular beam epitaxy (MBE). In this paper, we describe systematic experiments which indicate that the substrate treatment is crucial to the highly crystalline and uniform growth of one-dimensional nanomaterials. The influence of natural oxidation time on the crystallinity and uniformity of GaAs NW arrays was investigated and is discussed in detail. The GaAs NW crystallinity and uniformity are maximized after 20 days of natural oxidation time. This work provides a new solution for producing high-crystallinity uniform III–V nanowire arrays on wafer-scale Si substrates. The highly crystalline uniform NW arrays are expected to be useful for NW-based optical interconnects and Si platform optoelectronic devices.

Keywords: GaAs, nanowire arrays, self-catalyzed, molecular beam epitaxy

PACS: 61.46.–w, 07.79.Pk, 81.10.bk, 81.15.Hi **DOI:** 10.1088/1674-1056/abf920

1. Introduction

The III–V semiconductor nanowires (NWs) not only have the dimensional characteristics of one-dimensional materials, but also retain the good photoelectric properties of semiconductor materials. Nanomaterials exhibit superior electrical and optical properties at low-dimensional levels, and are utilized for electronic and photonic devices, including nanowire transistors,[1] nanolasers,[2,3] photodetectors,[4] light-emitting diodes,[5] solar cells,[6] and single-electron memory devices.[7] Vertically aligned NW arrays are widely used in optoelectronic devices, such as solar cells,[8,9] photodetectors,[10] light emitters[11] and for biological/chemical sensing[12,13] due to their high efficiency and potential sensitivity. Compared with conventional thin film devices, they have enhanced light absorption[14] and improved carrier collection efficiency.[15] Moreover, NW arrays also achieve good performance in thermoelectric devices, due to the high ratio of cross-sectional areas and device areas.[16] In order to introduce nano devices into practical applications, it is necessary to grow NW arrays with high density and uniformity.

Fabrication methods for Si-based vertically aligned NWs are numerous, including molecular beam epitaxy (MBE),[17–19] metal–organic vapor phase epitaxy (MOVPE)[20] and top-down fabrication methods using reactive ion etching (RIE).[21] As such, arrays of vertically aligned NWs can be obtained by substrate treatments, such as electron beam lithography,[22] nanoimprint lithography,[23] nanosphere lithography,[24] and laser interface lithography.[25] All of the above methods can increase the NWs' verticality by the use of patterned substrates. In addition, the control of NW density can be achieved by hole spacing. However, due to technical limitations, the growth of NWs by these methods involves a high cost, and is unsuitable for the preparation of large-area NW arrays and wafer-scale production. In our previous research, a chemical solution etching method was successfully used to fabricate GaAs NW arrays.[26] Due to the violent chemical reaction, there is still a lack of control of the surface state of the substrate and the crystal quality of the resulting materials. Therefore, a gentler way is needed to change the surface state of the substrate, so as to realize the preparation of high-crystallinity uniform GaAs NW arrays.

In this paper, we describe the growth of GaAs NWs on n-type Si (111) substrates using a self-catalyzed growth mechanism by molecular beam epitaxy (MBE). The morphology and crystallinity were studied using scanning electron microscopy (SEM) and x-ray diffraction (XRD). The natural oxidation of substrates is an effective way to obtain high-crystallinity uniform GaAs NW arrays. A natural oxidation time of 20 days represents the best conditions for obtaining high-crystallinity

*Project supported by the National Natural Science Foundation of China (Grant Nos. 61674021, 11674038, 61704011, 61904017, 11804335, and 12074045), the Developing Project of Science and Technology of Jilin Province, China (Grant No. 20200301052RQ), the Project of Education Department of Jilin Province, China (Grant No. JJKH20200763KJ), and the Youth Foundation of Changchun University of Science and Technology (Grant No. XQNJJ-2018-18).

†Corresponding author. E-mail: linfengyuan_0116@163.com
‡Corresponding author. E-mail: jl_tangcust@163.com

© 2021 Chinese Physical Society and IOP Publishing Ltd

uniform GaAs NW arrays with a verticality of 98.4% and an optimal GaAs (111) Bragg diffraction peak. This work promises a simple and effective way to fabricate large-area III–V semiconductor NW arrays on wafer-scale Si substrates.

2. Material and methods

All Si substrates surfaces were cleaned by ultrasonic with ethanol and deionized (DI) water cleaning. Sample A was ultrasonically cleaned with ethanol and deionized water for 5 min and then nitrogen blow dried. For sample B, compared to sample A, we first removed the native SiO_2 layer of sample B by 2 min of wet etching with diluted BOE (HF : DI = 1 : 10). The substrate was then ultrasonically processed for 5 min in an ethanol solution to remove the remains. Subsequently, we placed the dried substrate in a super-clean chamber at a temperature of 21 ± 0.5 °C and a humidity of 40% under natural oxidation for 10 days. In order to obtain high-crystallinity uniform GaAs NW arrays, we used the same treatment as for sample B. The Si substrates were naturally oxidized for 5, 15, 20, 25 and 30 days. Finally, the Si substrates were treated by the ultra-high vacuum environment of our MBE system (DCA P600).[26]

The self-catalyzed GaAs NWs were grown on n-type Si (111) substrates by MBE. Ga droplets were deposited on Si substrates at a beam equivalent pressure (BEP) of 6.2×10^{-8} Torr, using a deposition time of 35 s and a temperature of ~ 600 °C. The BEPs for group III and group V elements were measured by a beam flux monitor (BFM). Subsequently, GaAs NW arrays were grown with a Ga BEP of 6.2×10^{-8} Torr, an As BEP of 1.4×10^{-6} Torr and a V/III flux ratio of 22.5. The growth temperature was ~ 600 °C and the growth time was 30 min. After the growth, the Ga flux was switched off and the samples were cooled to 300 °C under As overpressure. Finally, the samples were naturally cooled to room temperature.

The morphology of the GaAs NWs was examined by scanning electron microscopy (SEM, HITACHI S-4800) system. The crystal quality of the GaAs NWs was determined by x-ray diffraction (XRD). XRD patterns were recorded in a 2θ range of 20–100° with an x-ray diffractometer (Model ULTIMA IV, Rigaku, Japan) using Cu $K\alpha$ radiation (λ = 1.5418 Å) as the x-ray source.

3. Results and discussion

The morphology of the GaAs NWs (sample A) was studied by SEM, as shown in Figs. 1(a) and 1(b). Most of the GaAs NWs are tilted with respect to the Si substrate, and sparsely distributed on the Si substrate. The verticality, density, average length and average diameter of sample A are 42.6%, 2.32×10^8 cm^{-2}, 1.68 μm and 86 nm, respectively. The morphology of the GaAs NWs grown on naturally oxidized Si substrate (sample B) is shown in Figs. 1(c) and 1(d). The GaAs NW arrays show higher verticality and density, at 95.8% and 5.63×10^8 cm^{-2}, respectively. Moreover, XRD measurements were carried out in order to further determine the crystallization of the GaAs NWs. Figures 1(e) and 1(f) show the XRD patterns of sample A (black curve) and sample B (10 days) (red curve). The XRD standard spectra of GaAs (cyan line) were verified using the Joint Committee on Powder Diffraction Standards (JCPDS) standard database. The full width at half maximum (FWHM) and Bragg diffraction peak intensity

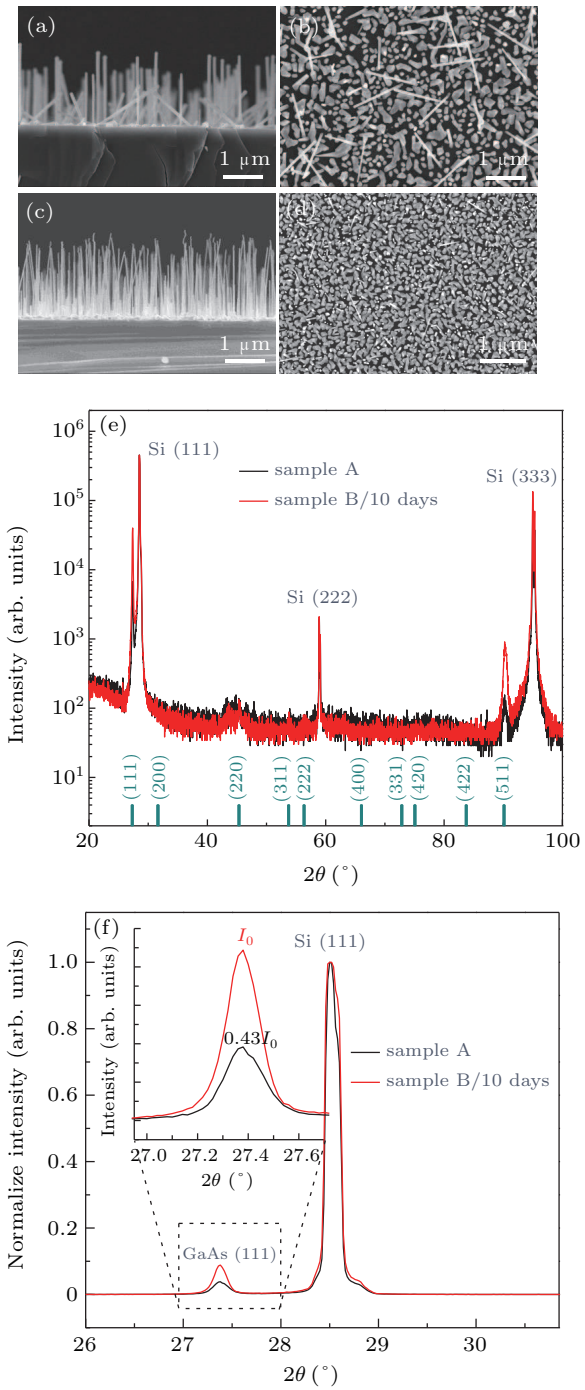


Fig. 1. SEM images of sample A, side view (a) and planar view (b). SEM images of sample B (10 days), side view (c) and planar view (d). (e, f) XRD patterns of sample A (black curve) and sample B (10 days) (red curve). The inset shows the GaAs (111) diffraction peak of samples A and B (10 days).

of XRD profiles are used to characterize different material crystallinities. The GaAs (111) diffraction peak intensity of sample B is denoted by I_0, and its FWHM is 0.155° . Furthermore, the GaAs (111) Bragg diffraction peak FWHM and intensity of sample A are 0.183° and $0.43I_0$, respectively. Based on a crystallinity comparison of the GaAs NWs obtained from the sample A and sample B above, it can be seen that Si substrate processing is essential for the growth of high-crystallinity NW arrays.

In addition, two morphologies of sample B (10 days) are shown in the inset of Fig. 2. One class of GaAs NWs is long and thin (defined as type-I), and the other class of GaAs NWs is short and coarse (defined as type-II). The lengths and diameters of type-I and type-II are shown in Fig. 2. The orange and purple histograms represent the lengths and diameters of type-I and type-II, respectively. The average length and diameter of type-I are 1.78 μm and 34 nm, and those of type-II are 0.87 μm and 48 nm, respectively. According to the morphological comparison of the GaAs NWs (samples A and B), it can be seen that Si substrate processing is significant for the growth of uniform NW arrays.

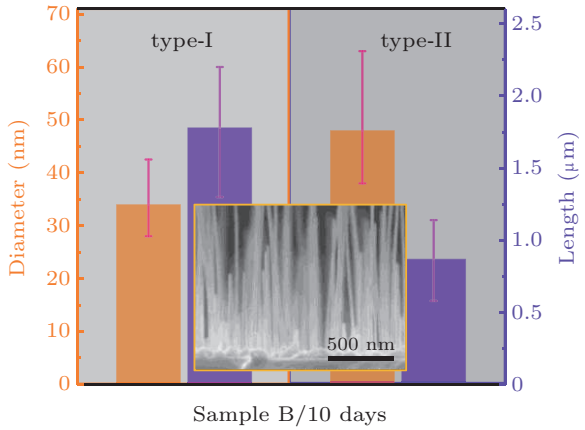


Fig. 2. Two morphologies of sample B (10 days), showing the length and diameter of sample B (10 days). The inset shows the morphology of sample B (10 days).

In order to obtain high-crystallinity uniform GaAs NW arrays, GaAs NWs were grown on Si substrates with different natural oxidation times. Figure 3 shows SEM images of GaAs NWs grown on Si substrates with different natural oxidation times. Among them, side views of GaAs NWs corresponding to natural oxidation times of 5, 10, 15, 20, 25 and 30 days are shown in Figs. 3(a)–3(f). Moreover, planar views of the six samples are shown in the inset of Figs. 3(a)–3(f). These images also indicates that naturally oxidized Si substrates can obtain highly vertical GaAs NW arrays. In order to better characterize the high-density uniform vertically aligned NW arrays, we measured the verticality, density, length and diameter of the GaAs NWs. The particle size distribution and density of all GaAs NWs were counted, and the number of GaAs NWs was not less than 200. The measurement results are shown in Table 1.

Table 1. The verticality, density, average length and diameter of GaAs NWs grown on Si substrates with different natural oxidation times.

Samples	Vertical (%)	Density (10^8 cm^{-2})	Average length (μm)	Average diameter (nm)
5 days	98	2.69	0.53	150
10 days	95.8	5.63	1.78/0.87	34/48
15 days	96.8	6.65	1.8/0.91	30/45
20 days	98.4	7.3	1.82	41
25 days	94.6	5.96	1.84	36
30 days	100	2.24	1.45	30

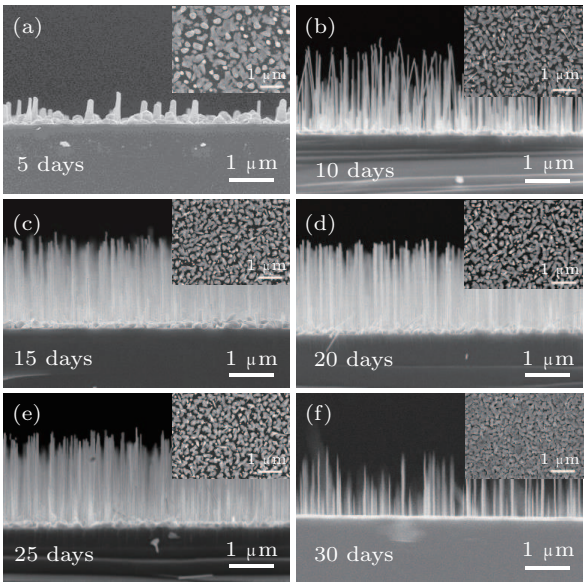


Fig. 3. GaAs NW growth on substrates with different natural oxidation times. SEM images of samples oxidized for 5 days, side view (a); 10 days, side view (b); 15 days, side view (c); 20 days, side view (d); 25 days, side view (e); 30 days, side view (f). The insets show the planar views of the six samples.

In addition, in order to observe the verticality and density of the GaAs NWs more intuitively, the distribution of vertical and density with natural oxidation time were plotted, as shown in Fig. 4(a). Overall, most of the GaAs NWs grown on the natural-oxidation Si substrate were vertically aligned; the verticality of the NWs exceeded 95%. Figure 4(a) shows that the density of GaAs NWs first increases and then decreases with oxidation time, and that at an oxidation time is 20 days, the density of NWs is maximized, reaching 7.3×10^8 cm^{-2}. When the oxidation time is 20 days, the verticality of the vertically aligned GaAs NWs is 98.4%. The inset orange rectangle of Fig. 4(a) shows the morphology of GaAs NWs grown on the naturally oxidized Si substrate after 20 days. Compared with sample B of GaAs NWs grown on a naturally oxidized Si substrate for 10 days, the morphology of the GaAs NWs grown on the naturally oxidized Si substrate for 20 days is more uniform. To provide a further determination of the optimal conditions for uniform GaAs NWs, a distribution histogram of length and diameter with natural oxidation time was plotted, as shown in Fig. 4(b). The morphology of GaAs NWs grown on the naturally oxidized Si substrate for 5 days is short and coarse. GaAs NWs grown on the naturally oxidized Si

substrate for 10 and 15 days show two morphologies. With an increase in the natural oxidation time, uniform GaAs NWs were grown. As a result, we find that the optimal growth conditions for obtaining high-density vertically aligned uniform GaAs NW arrays grown on a Si substrate is a natural oxidation period of 20 days.

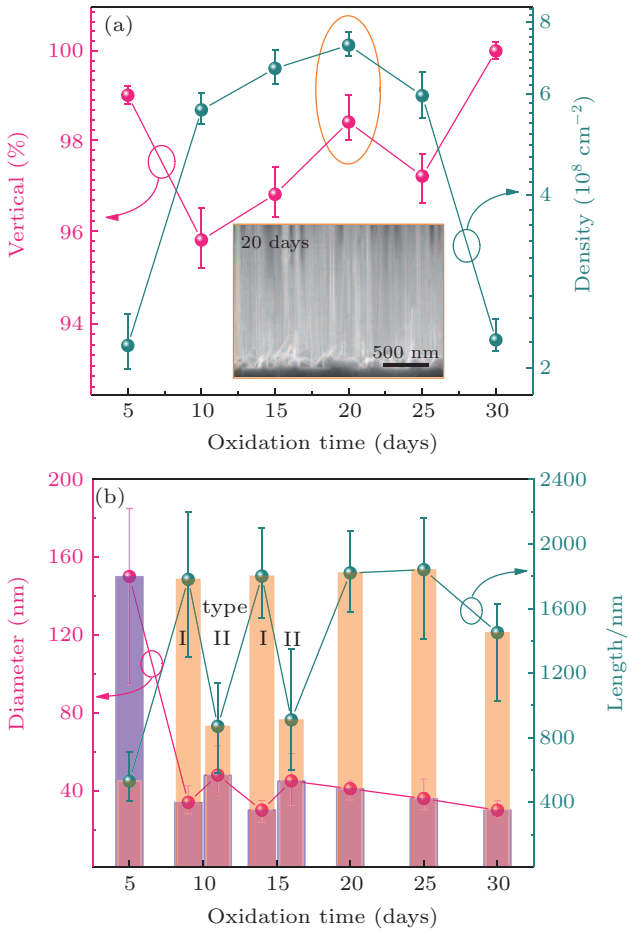


Fig. 4. (a) The verticality and density distribution of GaAs NWs grown on Si substrates with different natural oxidation time. The inset shows the morphology of GaAs NWs grown on Si substrates for 20 days. (b) The length and diameter distribution of GaAs NWs grown on Si substrates with different natural oxidation time.

In order to better determine the effects of natural oxidation time on the crystalline quality of the GaAs NW arrays, the samples were characterized by XRD, as shown in Fig. 5. All the diffraction peaks were identified using the JCPDS standard database. The XRD spectra show that the Bragg diffraction peaks of GaAs are similar for the six samples, as shown in Fig. 5(a). Figure 5(a) shows that GaAs (111) is the main diffraction peak in GaAs NWs. In contrast, the FWHM and diffraction peak intensity of the GaAs diffraction peaks are different for the six samples, as shown in Fig. 5(b). With an increase in the natural oxidation time, the GaAs (111) Bragg diffraction peak position is constant and the peak strength is obviously different, as shown in the inset of Fig. 5(b). The FWHM and diffraction peak intensity of the GaAs (111) Bragg diffraction peaks are shown in Fig. 5(c). Figure 5(c) shows that with an increase in the natural oxidation time, the FWHM of the GaAs (111) Bragg diffraction peak first decreases and then increases; at an oxidation time of 20 days, it reaches a minimum. Meanwhile, the intensity of the GaAs (111) Bragg diffraction peak first increases and then decreases; the natural oxidation time required to reach the maximum is 20 days. As a result, we can state that the optimal growth condition for obtaining high-crystallinity uniform GaAs NW arrays grown on Si substrate is the natural oxidation time of 20 days.

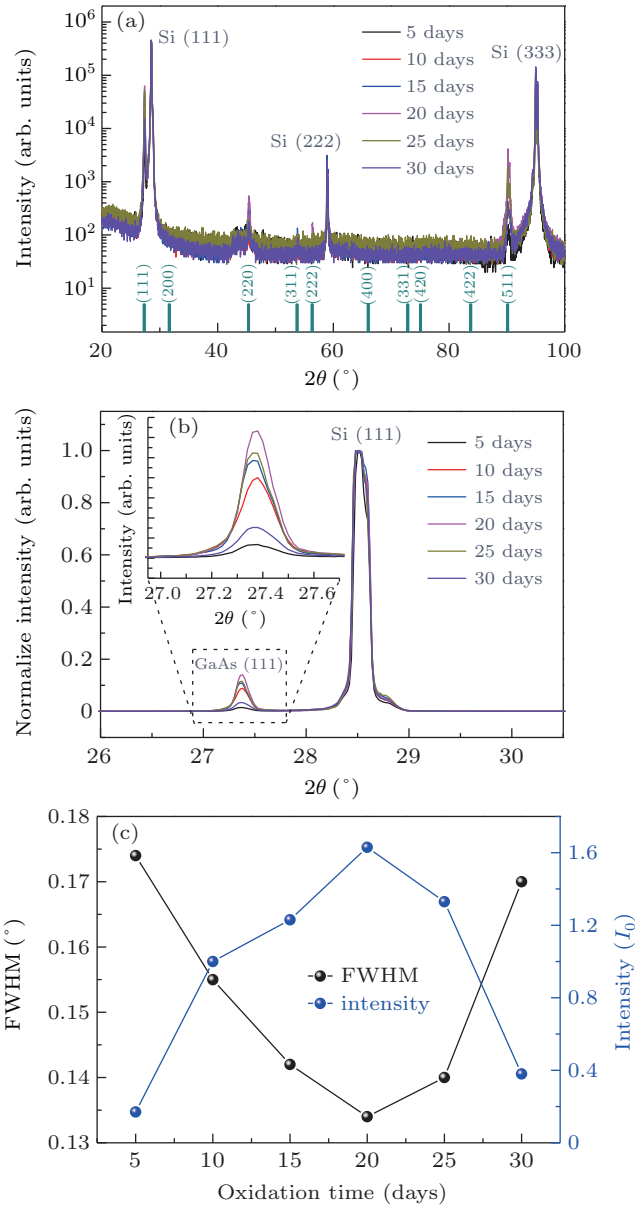


Fig. 5. (a) XRD patterns of GaAs NWs and (b) GaAs (111) Bragg diffraction peaks with different natural oxidation time. The inset shows the GaAs (111) diffraction peaks of the six samples. (c) FWHM and diffraction peak intensity of GaAs (111) Bragg peaks with different natural oxidation time.

4. Conclusion

In conclusion, we have demonstrated the natural oxidation patterned self-catalyzed growth of high-crystallinity uniform GaAs NW arrays on n-type Si (111) substrates by MBE. The influence of the natural oxidation time on the morphology and crystallinity of GaAs NW arrays was studied and dis-

cussed in detail. The morphology and crystallinity of the GaAs NW arrays were studied by SEM and XRD, and we then determined the best conditions for handling the substrate. When the natural oxidation time is 20 days, the GaAs NW uniformity is optimized. Meanwhile, the FWHM and the intensity of GaAs (111) Bragg diffraction peak are minimized and maximized, respectively. A simple and effective fabrication method for high-crystallinity uniform III–V NW arrays on wafer-scale Si substrates for various device applications is to be expected.

References

[1] Tomioka K, Yoshimura M and Fukui T 2012 *Nature* **488** 189

[2] Saxena D, Mokkapati S, Parkinson P, Jiang N, Gao Q, Tan H H and Jagadish C 2013 *Nat. Photon.* **7** 963

[3] Li H L, Chen Y T, Wei Z P and Chen R 2020 *Sci. China Mater.* **63** 1364

[4] Zhu X T, Lin F Y, Zhang Z H, Chen X, Huang H, Wang D K, Tang J L, Fang X, Fang D, Ho J C, Liao L and Wei Z P 2020 *Nano Lett.* **20** 2654

[5] Dimakis E, Jahn U, Ramsteiner M, Tahraoui A, Grandal J, Kong X, Marquardt O, Trampert A, Riechert H and Geelhaar L 2014 *Nano Lett.* **14** 2604

[6] Holm J V, Jorgensen H I, Krogstrup P, Nygard J, Liu H Y and Aagesen M 2013 *Nat. Commun.* **4** 1498

[7] Thelander C, Nilsson H A, Jensen L E and Samuelson L 2005 *Nano Lett.* **5** 635

[8] Wang Y, Zhang Y, Zhang D, He S and Li X 2015 *Nanoscale Res. Lett.* **10** 269

[9] Liang D, Kang Y S, Huo Y J, Chen Y S, Cui Y and Harris J S 2013 *Nano Lett.* **13** 4850

[10] Chen G, Liang B, Liu Z, Yu G, Xie X M, Luo T, Xie Z, Chen D, Zhu M Q and Shen G Z 2014 *J. Mater. Chem. C* **2** 1270

[11] Tomioka K, Motohisa J, Hara S, Hiruma K and Fukui T 2010 *Nano Lett.* **10** 1639

[12] Engel Y, Elnathan R, Pevzner A, Davidi G, Flaxer E and Patolsky F 2010 *Angew. Chem. Int. Ed.* **49** 6830

[13] Rostgaard K R, Frederiksen R S, Liu Y C, Berthing T, Madsen M H, Holm J, Nygard J and Martinez K L 2013 *Nanoscale* **5** 10226

[14] Hu L and Chen G 2007 *Nano Lett.* **7** 3249

[15] Kelzenberg M D, Boettcher S W, Petykiewicz J A, Turner-Evans D B, Putnam M C, Warren E L, Spurgeon J M, Briggs R M, Lewis N S and Atwater H A 2010 *Nat. Mater.* **9** 239

[16] Zhang T, Wu S, Zheng R and Cheng G 2015 *Nano Energy* **13** 433

[17] Yu X Z, Li L X, Wang H L, Xiao J X, Shen C, Pan D and Zhao J H 2016 *Nanoscale* **8** 10615

[18] Matteini F, Tütüncüoglu G, Potts H, Jabeen F and Fontcuberta i Morral A 2015 *Cryst. Growth Des.* **15** 3105

[19] Cohin Y, Mauguin O, Largeau L, Patriarche G, Glas F, Sondergard E and Harmand J C 2013 *Nano Lett.* **13** 2743

[20] Dick K A, Deppert K, Martensson T, Mandl B, Samuelson L and Seifert W 2005 *Nano Lett.* **5** 761

[21] Fu Y Q, Colli A, Fasoli A, Luo J K, Flewitt A J, Ferrari A C, Milne W I 2009 *J. Vac. Sci. Technol. B* **27** 1520

[22] Dubrovskii V G, Xu T, Álvarez A D, Plissard S R, Caroff P, Glas F and Grandidier B 2015 *Nano Lett.* **15** 5580

[23] Munshi A M, Dheeraj D, Fauske V T, Kim D C, Huh J, Reinertsen J F, Ahtapodov L, Lee K D, Heidari B, van Helvoort A T J, Fimland B and Weman H 2014 *Nano Lett.* **14** 960

[24] Fuhrmann B, Leipner H S, Höche H R, Schubert L, Werner P and Gösele U 2005 *Nano Lett.* **5** 2524

[25] Kim D S, Ji R, Fan H J, Bertram F, Scholz R, Dadgar A, Nielsch K, Krost A, Christen J, Gosele U and Zacharias M 2007 *Small* **3** 76

[26] Kang Y B, Tang J L, Wang P H, Lin F Y, Fang X, Fang D, Wang D K, Wang X H and Wei Z P 2018 *Mater. Res. Express* **6** 035012